4th Theoretical Fluid Mechanics Meeting, June 6-9, Toronto

Quasi-Simultaneous Viscous-Inviscid Interaction for Transonic Airfoil Flow

Arthur E.P. Veldman*

University of Groningen, Groningen, The Netherlands

Following Prandtl, a viscous-inviscid interaction (VII) method is presented, where the flow field is divided into a viscous shear layer and an inviscid outer region. Their coupling is performed with the quasi-simultaneous approach, making use of an appropriately chosen interaction law. Firstly, an engineering example of transonic airfoil flow is presented, in which the interaction law is based on thin-airfoil theory. Thereafter, the VII coupling approach is analyzed by mathematical means, leading to a strongly simplified interaction law, yet allowing calculations beyond maximum lift simply starting from scratch.

I. Introduction

When simulating flow around aircraft, one of the physical phenomena to be considered is viscosity. In transonic cruise conditions it can reduce the lift by as much as 50% when compared to a purely inviscid situation.[1] Also, viscosity plays a role in take-off and landing performance: it determines, for instance, the maximum lift which can be achieved. In many cases viscosity plays its role only in a thin shear layer, consisting of boundary layer and wake, whereas the remaining part of the flow field can be considered inviscid. Thus a subdivision of the flow field is created (Fig. 1), with different models for each of the two regions. Coupling the models, a so-called Viscous-Inviscid Interaction (VII) method is obtained. The price of a simulation with a VII method is, of course, higher than the price for a simulation based on an inviscid-flow model. However, its price is much less than the price to be paid for a simulation based on a Navier–Stokes approach.[2]

In VII methods, the shear layer is usually modelled through the boundary-layer equations, be it in differential or integral form. The paper shortly describes the modelling of the viscous and inviscid flow regions, respectively. The emphasis is on the coupling between the two subdomains, i.e. on the numerical treatment of the viscous-inviscid interaction process. In particular the quasi-simultaneous VII approach will be highlighted.

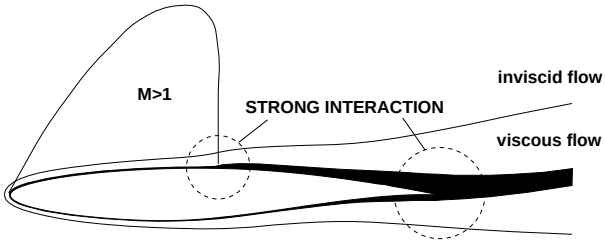

Figure 1. Subdivision of flow field in viscous shear layer and inviscid-flow region (shear layer exaggerated in thickness).

Examples are presented from transonic flow around the RAE2822 airfoil, for which experimental data are available. In these examples the quasi-simultaneous interaction law is chosen relatively close to the physics, making its implementation somewhat complicated. Therefore, also ideas are presented on simplifying the interaction law. In fact, the resulting method is very close to the direct interaction method which breaks down in separation. Nevertheless, it turns out te be very robust, and is able to simulate airfoil flow beyond maximum lift from scratch (i.e. without needing a good initial guess).

*Professor, Institute of Mathematics and Computing Science, P.O. Box 800, 9700 AV Groningen, AIAA member.

II. Mathematical model

In this section a short description is given of the flow models in the viscous shear layer (boundary layer and wake) and in the inviscid flow, respectively. Also their mathematical coupling is described.

A. Viscous-flow boundary-value problem

The boundary layer and wake are described with a field method, which in principle offers the possibility to apply refined turbulence modelling. When the development of this method, called VISIAN, began (in the late 1970s at the National Aerospace Laboratory NLR) it was hoped that within a few years more sophisticated flow models would become available. However, turbulent-flow modelling turned more complicated than expected.

In a field method, the non-dimensional equations of motion in the shear layer read

$$\text{continuity:} \qquad \frac{\partial}{\partial x}(\rho u) + \frac{\partial}{\partial y}(\rho v) = 0; \tag{1}$$

$$x\text{-momentum:} \qquad u\frac{\partial u}{\partial x} + v\frac{\partial u}{\partial y} = -\frac{1}{\rho}\frac{\partial p}{\partial x} + \frac{\partial}{\partial y}\left(\mu_{\text{ef}}\frac{\partial u}{\partial y}\right). \tag{2}$$

Here u and v are the velocity components along the airfoil surface and perpendicular to it, respectively (the (x, y)-coordinate system). Further, ρ is the density, p is the pressure and μ_{ef} is the effective viscosity containing the influence of turbulence. For scaling of the variables, the upstream values have been used, together with a characteristic length.

The shear-layer equations are solved subject to boundary conditions at the airfoil surface $y = 0$ where the velocity vanishes, and at the edge of the shear layer $y = y_e$ where the edge values u_e and p_e follow from a match with the inviscid flow (Section C). In the wake the vertical velocity along the cut $y = 0$ follows from the position of the dividing inviscid-flow streamline.

In first-order boundary-layer theory, as used here, the pressure is assumed to be constant across the shear layer. But here this pressure level is allowed to differ from the inviscid-flow pressure; this difference represents the influence of streamline curvature (Section C). The flow in the shear layer is assumed compressible, with the temperature described from Crocco's integral energy equation. Pressure, density and Mach number are modelled through relations for isentropic flow with constant total enthalpy. The influence of turbulence is modeled by means of the algebraic eddy-viscosity model of Cebeci and Smith, with an extension in the wake as introduced by Cebeci et al.[3]

B. Inviscid-flow boundary-value problem

The inviscid flow is formulated in terms of the full-potential equation in mass-conservation form

$$\frac{\partial}{\partial x}\left(\rho\,\frac{\partial \Phi}{\partial x}\right) + \frac{\partial}{\partial y}\left(\rho\,\frac{\partial \Phi}{\partial y}\right) = 0, \tag{3}$$

where the density

$$\rho = \left\{1 + \frac{\gamma-1}{2}M_\infty^2\left[1 - \left(\frac{\partial \Phi}{\partial x}\right)^2 - \left(\frac{\partial \Phi}{\partial y}\right)^2\right]\right\}^{1/(\gamma-1)}$$

is nondimensionalized by the upstream value ρ_∞, and M_∞ is the (subsonic) Mach number of the upstream flow. Details of the method, called TRAFS, can be found in Ref. 4.

At the airfoil surface the normal mass outflux is given as a transpiration condition

$$\rho\Phi_n = \rho_0 v_0, \tag{4}$$

where Φ_n is the component of the potential-flow velocity in the direction normal to the airfoil. The displacement and curvature effects of the viscous wake are represented in the potential flow by specifying jumps in normal mass flux $\rho\Phi_n$ and tangential velocity Φ_t:

$$\begin{aligned} (\rho\Phi_n)_u - (\rho\Phi_n)_\ell &= (\rho_0 v_0)_u - (\rho_0 v_0)_\ell, \\ (\Phi_t)_u - (\Phi_t)_\ell &= (u_0)_u - (u_0)_\ell. \end{aligned} \tag{5}$$

The subscripts u and ℓ refer to the upper and lower side of the wake cut.

The problem to compute the potential flow is equivalent to that of solving the boundary-value problem defined by Eqs. (3) – (5) for the unknown potential Φ; either at prescribed angle-of-attack or at prescribed lift. The potential flow becomes unique if the velocity components are required to remain finite at the trailing edge point (Kutta condition), which can be formulated more precisely by demanding that the second jump condition in Eq. (5) is also valid in the trailing edge.

C. Coupled boundary-value problem

The two boundary-value problems described above are coupled by demanding continuity of the flow variables at the edge of the shear layer. Usually the resulting relation is transformed into a relation between inviscid-flow variables at the matching surface (denoted by the subscript '0') and viscous-flow variables at the edge of the shear layer (denoted by the subscript 'e'). In physical terms, these relations describe the displacement effect of the shear layer (translated into a mass outflow), and the effect of streamline curvature (translated into a pressure jump).

Displacement effect The displacement effect of the shear layer is formulated as a surface transpiration condition. Along the airfoil it reads

$$\rho_0 v_0 = \frac{\mathrm{d}}{\mathrm{d}x}(\rho_e u_e \delta^*), \tag{6}$$

where δ^* is the displacement thickness. The wake is split in two parts, according to the wake cut $y = 0$; similar relations hold here.

Streamline curvature The effect of streamline curvature can be modelled as a jump between the pressure p_0 from the outer inviscid flow and the pressure level p_e in the boundary layer[5]

$$p_0 - p_e = \rho_e u_e \kappa(\theta + \delta^*). \tag{7}$$

Here, θ denotes the momentum thickness, whereas κ denotes the streamline curvature estimated by

$$\kappa = \kappa_w + \frac{\mathrm{d}^2}{\mathrm{d}s^2}(\delta^*) \tag{8}$$

(κ_w is the curvature of the wall). In the wake similar relations hold for upper and lower side, respectively. Note that the linearized Bernoulli equation transforms these pressure jumps into jumps between the inviscid and viscous streamwise velocities, u_0 and u_e, respectively.

III. Viscous-inviscid interaction

A. The quasi-simultaneous method

Following Prandtl, the boundary-layer equations are usually solved with prescribed pressure. However, in points of flow separation such an approach leads to (numerical) problems, in fact a total breakdown of the calculations results. An extensive study of these problems, presented by Goldstein in 1948,[6] suggested several possible causes for this breakdown. One of his suggestions was that the problem could originate in the prescribed pressure, which should satisfy certain conditions. Twenty years later, Catherall and Mangler[7] indeed showed that when prescribing displacement thickness, the shear-layer equations can be integrated through the separation point. At the same time, Stewartson in the UK,[8] Neiland in the USSR[10] and Messiter in the USA[9] came up with the concept of the triple deck. Its most important property is that there exists no hierarchy[11] between shear layer and inviscid flow near singular points (such as a point of flow separation): *strong interaction*.

The situation near a point of flow separation can be described as follows. By varying a prescribed displacement thickness δ^* at a given boundary-layer station it is possible to study the behaviour of the streamwise velocity u_e. A typical situation is sketched in Fig. 2. The essential feature of this graph is that u_e possesses a minimum, which is found to correspond with the onset of flow separation. As Goldstein already hunched, no boundary-layer solution will exist for values of u_e below this minimum. On the other hand, prescription of δ^* or a suitable combination of u_e and δ^* will lead to a solution of the boundary-layer equations.

Based on these findings, in the late 1970s a number of proposals have been made to solve viscous-inviscid interaction problems. The first proposal, simply inverting the order of information between invisicd flow and shear layer,[12] did survive in flow separation but possessed very bad convergence properties. A better idea was to mix the classical direct approach and the inverse approach into the semi-inverse method.[13,14] This method has become quite powerful in engineering applications.[15]

At NLR another approach was followed, inspired by the lack of hierarchy between both flow regions; the idea was to solve them simultaneously.[16,17] However, at that time computers were quite modest (only 1 Mb of central memory), and a full simultaneous treatment was impossible (except when using integral methods[18,19,20]). But one could try to approach such an idea. For instance by solving the shear layer equations together with a simple approximation of the outer flow that contained the essential part of the interaction. As triple-deck theory showed that the local invisicd-flow interaction is described by thin-airfoil theory, the quasi-simultaneous method was born.

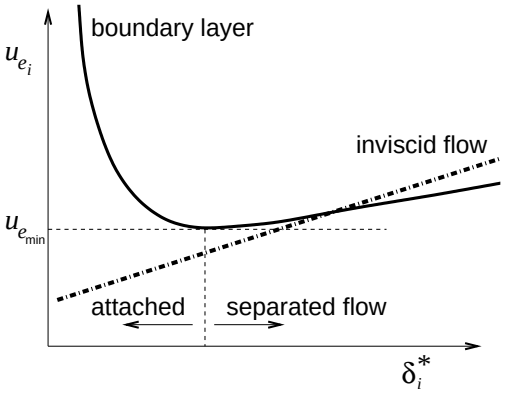

Figure 2. A sketch of the boundary-layer behaviour, combined with an inviscid-flow relation.

The quasi-simultaneous method is easily explained in abstract terms by first defining the external inviscid-flow operator $u_e = E_u[\delta^*]$ and boundary-layer operator $u_e = B[\delta^*]$. Further, the approximate inviscid-flow description is denoted by $u_e = I[\delta^*]$; it is called the interaction law. With this notation, the quasi-simultaneous method can be written as

$$\begin{aligned} u_e^{(n)} - I[\delta^{*(n)}] &= E_u[\delta^{*(n-1)}] - I[\delta^{*(n-1)}], \\ u_e^{(n)} - B[\delta^{*(n)}] &= 0. \end{aligned} \tag{9}$$

It is stressed that the interaction law is used in defect formulation, i.e. it does not influence the final result of the calculations. It is however very important for letting the calculations survive during all iterations on their way to the final flow solution.

The interaction law From the local asymptotic descriptions of strong interaction, it is natural to base the interaction law on thin-airfoil theory. Here, the airfoil is considered to be a flat segment, located at the interval $[0, c]$ of the x-axis of a Cartesian coordinate system (x, y). Let u and v, generically, denote the velocity components, and let their symmetric and antisymmetric parts be indicated by the subscripts s and a, respectively. Then the following thin-airfoil formulas, which are continuous in the trailing edge, form the basis of the interaction law:

- *symmetric* $(0 \le x < \infty)$

$$u_s(x) = \frac{1}{\pi} \int_0^\infty v_s(\xi) \frac{\mathrm{d}\xi}{x - \xi}; \tag{10}$$

- *antisymmetric at the profile* $(0 \le x < c)$

$$u_a(x) = \frac{1}{\pi} \sqrt{\frac{c-x}{x}} \left[\int_0^c \sqrt{\frac{\xi}{c-\xi}}\, v_a(\xi) \frac{\mathrm{d}\xi}{x-\xi} - \int_c^\infty \sqrt{\frac{\xi}{\xi-c}}\, u_a(\xi) \frac{\mathrm{d}\xi}{x-\xi} \right]; \tag{11}$$

- *antisymmetric in the wake* $(c < x < \infty)$

$$v_a(x) = \frac{1}{\pi} \sqrt{\frac{x-c}{x}} \left[\int_0^c \sqrt{\frac{\xi}{c-\xi}}\, v_a(\xi) \frac{\mathrm{d}\xi}{x-\xi} + \int_c^\infty \sqrt{\frac{\xi}{\xi-c}}\, u_a(\xi) \frac{\mathrm{d}\xi}{x-\xi} \right]. \tag{12}$$

In the trailing edge $(x = c)$ the antisymmetric formula (11) degenerates into $u_a(c) = \lim_{\xi \downarrow c} u_a(\xi)$. Its right-hand side is calculated from the jumps in u on upper and lower side of the trailing edge $u_a(c) = \frac{1}{2}([u]_{u,te} - [u]_{\ell,te})$. Note that this formulation is equivalent with using a Kutta condition, which imposes continuity of the pressure in the trailing edge, i.e. $p_{e,u} = p_{e,\ell}$.

To incorporate the effects of compressibility, a Prandtl-Glauert transformation is applied to the equations above. This is easily accomplished by replacing the vertical velocity v according to

$$v \mapsto v(1 - M_\infty^2)^{-1/2}.$$

Remark: In Section V we will look for a simplification of the above formulas.

B. Inclusion of streamline curvature

Especially for rear-loaded airfoils the streamlines immediately behind the trailing edge are highly curved. In such a situation the assumption of constant pressure across the boundary layer is no longer justifiable *a priori*. The effect of streamline curvature can be modelled by a jump (7) between the pressure in the boundary layer p_e and the pressure of the inviscid flow $p_0 \equiv E_p[\delta^*]$:

$$p_e = E_p[\delta^*] - [p] \quad \text{with} \quad [p] = \kappa \rho_e u_e^2 (\delta^* + \theta). \tag{13}$$

The extended version of Eq. (9) thus *could* become

$$\begin{aligned} p_e^{(n)} - I_p[\delta^{*(n)}] &= E_p[\delta^{*(n-1)}] - [p]^{(n-1)} - I_p[\delta^{*(n-1)}], \\ p_e^{(n)} - B_p[\delta^{*(n)}] &= 0. \end{aligned} \tag{14}$$

Note that in Eq. (14) the pressure jump (13) is calculated from the previous iteration! This pressure jump is proportional to κ, which can be taken as the curvature of the displacement body given by Eq. (8). Thus the pressure jump scales with the 'second derivative' of the streamlines and herewith it introduces a strong-interaction character, as will be explained next.

When the pressure jump is evaluated from a previous iteration as indicated in Eq. (14), through κ, in the discretization of the second derivative of the displacement body it generates a contribution to the iterative amplification factor proportional to $(\delta x)^{-2}$, where δx is the mesh size. Letting the mesh size approach zero, this amplification blows up. This explains the numerical difficulties encountered in the literature when the curvature effect is not treated in a simultaneous way; see Ref. 5 (page 82). Extensive smoothing and underrelaxation is then required in order to obtain convergence of the viscous-inviscid iterations, as stated in Ref. 21 and references therein.

Once again, a simultaneous treatment of the curvature effect is required. The term $[p]^{(n-1)}$ should be shifted to the left-hand side in Eq. (14) and evaluated at the new iteration level (n). However, this necessary step to obtain convergence for small grid size turns out not to be sufficient. There is another (delicate) issue, which can be understood through a generalization of the analysis in Ref. 22. Let's assume that the curvature is computed from the displacement body, i.e. $\kappa = \mathrm{d}^2\delta^*/\mathrm{d}x^2$. Then the pressure jump (13) becomes

$$[p] = \rho_e u_e^2 (\delta^* + \theta) \frac{\mathrm{d}^2 \delta^*}{\mathrm{d}x^2} \quad \text{to be abbreviated as} \quad [p] = c \frac{\mathrm{d}^2 \delta^*}{\mathrm{d}x^2}.$$

The quasi-simultaneous system (14) now reads

$$\begin{aligned} p_e^{(n)} - I_p[\delta^{*(n)}] + c\frac{\mathrm{d}^2}{\mathrm{d}x^2}\delta^{*(n)} &= E_p[\delta^{*(n-1)}] - I_p[\delta^{*(n-1)}], \\ p_e^{(n)} - B_p[\delta^{*(n)}] &= 0. \end{aligned} \tag{15}$$

Since both I_p and $\mathrm{d}^2/\mathrm{d}x^2$ are negative-(semi)definite operators, and since $c > 0$, the two operators mentioned counteract each other in the left-hand side of Eq. (15)! Moreover, since the discrete version of I_p scales with $(\delta x)^{-1}$, whereas the curvature term scales with $(\delta x)^{-2}$, the unfavorable influence of the latter can be made arbitrary large for vanishing grid size. The envisaged iterations will not converge, and there is only one way out of this problem: discretize the second derivative with a one-sided expression

$$\left.\frac{\mathrm{d}^2 \delta^*}{\mathrm{d}x^2}\right|_i = \frac{\delta^*_{i-2} - 2\delta^*_{i-1} + \delta^*_i}{(\delta x)^2} \tag{16}$$

(the downstream-biased version will also work). At least in this way the eigenvalues of the discrete operator in Eq. (16) are positive, and hence of the same sign as those of $-I_p$. Numerical experiments with the usual

central discretization of the second derivative and with the above upstream-biased one have consistently revealed that only the latter one could be made convergent (at least for not too violent flow cases, which probably is related to the onset of wake instability – more research is required here). More information can be found in Refs. 23 and 24.

IV. Results

In previous publications[25,26] results of the combined VII method, called VISTRAFS, have been presented for various airfoils and compared with experiments and results of other flow simulation methods. Pressure variations across the shear layer due to the streamline curvature were not yet accounted for in those calculations. In the present paper, the results do include the influence of the normal pressure gradient by means of the pressure jump as described in Section B.

For rear-loaded airfoils the normal pressure gradient is expected to influence the calculated airfoil performance; therefore the RAE2822 airfoil has been selected for presentation of results. Flow conditions have been chosen for which extensive comparisons with the literature can be made (Table 1).

Table 1. Experimental data of selected flow cases for RAE 2822 airfoil.

	M_∞	Re	trip	α_{exp}	α_{corr}	C_L
Case 1	0.676	5.7×10^6	0.11	2.40	1.93	0.566
Case 6	0.725	6.5×10^6	0.03	2.92	2.44	0.743
Case 9	0.730	6.5×10^6	0.03	3.19	2.79	0.803

A. Numerics

In TRAFS an O-type grid with 129×65 grid points has been employed. In VISIAN a non-uniform C-type grid consisting of 193×21 grid points has been used, with 129 points along the airfoil surface. Per call of VISIAN 3 global marching sweeps through the shear layer were performed. Per shear-layer station, the Newton iterations are converged until 5 digits accuracy.

For situations with shock waves the prescription of the lift turns out to be more convenient. When the angle-of-attack is prescribed there is a danger of a limit cycle in the convergence behaviour, which is caused by the shock switching to and fro between two adjacent grid cells. The convergence rate is similar in both cases, but the iterations will not reach machine level.

The convergence behaviour of the iterations between VISIAN and TRAFS is presented in Fig. 3. It gives the difference between successive u_0 values. Case 1 has been calculated with α prescribed; for Cases 6 and 9 C_L was prescribed. The calculations shown have been performed in one consecutive run, with 15 iterations per flow case which is sufficient to approach machine zero (32-bit word length).

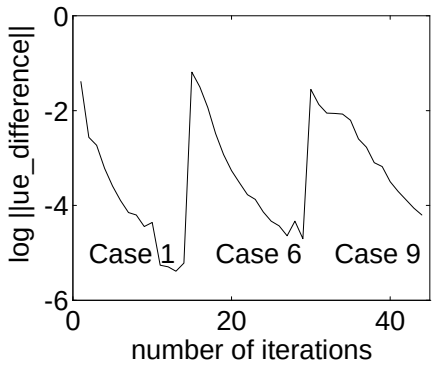

Figure 3. Convergence of u_e in viscous-inviscid iterations

For Case 1, with subsonic flow, 7 iterations are sufficient to reach the level $||\Delta u_e|| < 10^{-4}$. For Case 6, with transonic flow featuring a modest shock wave, 10 iterations are required to reach this level of convergence; Case 9, which exhibits some shock-induced flow separation, requires 13 iterations. The convergence rate for this case again is somewhat slower than for the preceding case. This can be explained, since the difference between the subsonic interaction law and the 'real' inviscid-flow model (i.e. TRAFS) becomes larger when the shock gets stronger. On current PC's it is not an issue to discuss CPU times: it is about 5 seconds per flow case.

Essential for the convergence of the viscous-inviscid iterations is that the pressure jump is treated simultaneously with the innermost iteration loop of VISIAN (see Section B). In the literature, numerical smoothing of the pressure jump is often reported to be necessary in order to obtain converged results.[21] This leads to an underestimation of the pressure jump, and it introduces a certain degree of arbitrariness

in the results, as explained in Ref. 5 (page 82). With the current approach there is no need for this kind of smoothing.

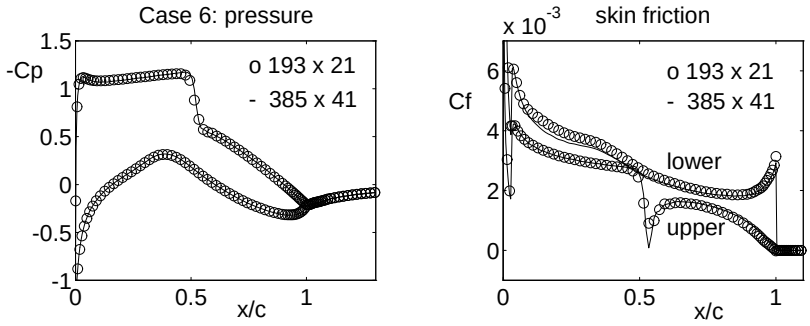

Figure 4. Grid refinement study (pressure and skin friction) for RAE2822 - Case 6.

To get an impression of the discretization error, the calculation of Case 6 has been repeated on a much finer grid: in VISIAN 385×41 (with 257 points along the profile) and in TRAFS 257×97. Figure 4 shows a comparison of the corresponding pressure and skin friction distributions; they are almost indistinguishable. The convergence rate of the viscous-inviscid iterations appears not to be affected by the grid refinement. This confirms the expectations: in both flow regions the calculations are converged sufficiently such that information about updated coupling conditions can spread across the whole flow domain. Even when one of the solvers is replaced by another one, the same VII convergence rate will be obtained.

B. Physics

Table 2 gives the aerodynamic coefficients (for grids with 129 points along the airfoil), with and without inclusion of the normal pressure gradient. For all cases, inclusion of the normal pressure gradient has a decreasing effect on the calculated lift, or an increasing effect on the computed angle-of-attack, respectively. This is consistent (although less outspoken) with the expectations for rear-loaded airfoils.[1,5]

Table 2. Experimental and calculated aerodynamic coefficients for RAE2822 airfoil.

	experiment				$[p] = 0$			$[p] \neq 0$		
	α_{exp}	C_L	C_D	α_{corr}	α	C_L	C_D	α	C_L	C_D
Case 1	2.40	0.566	0.0085	1.93	1.93	.589	0.0080	1.93	.581	0.0081
Case 6	2.92	0.743	0.0127	2.44	2.39	.743	0.0104	2.44	.743	0.0107
Case 9	3.19	0.803	0.0168	2.79	2.85	.803	0.0146	2.86	.803	0.0149

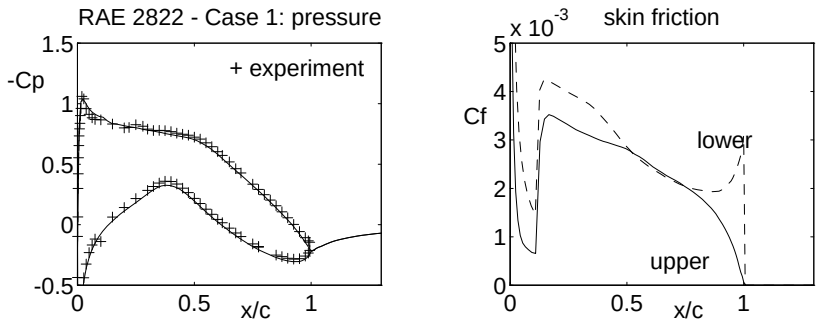

Figure 5. Pressure and skin friction for RAE2822 - Case 1.

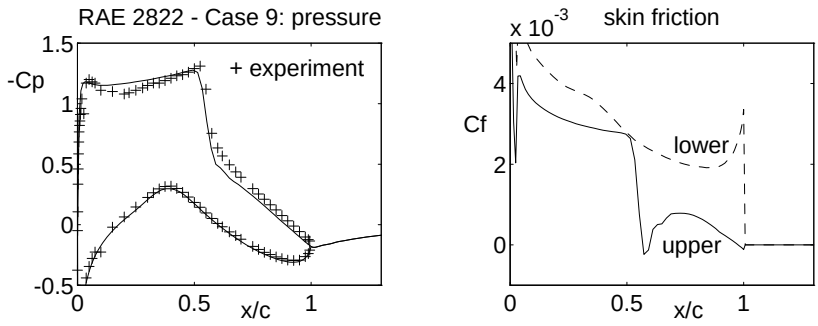

Figure 6. Pressure and skin friction for RAE2822 - Case 9.

In Figs. 5 and 6 we show the pressure (including experiment) and skin friction for Cases 1 and 9. The displacement thickness (Fig 7 (left)) shows a sharp kink at the trailing edge, which however does exactly fit to the kink due to the finite trailing edge angle. We demonstrate this in Fig. 7 (right), where for Case 9 the displacement body is shown. The curve is smooth: it is hardly possible to recognize individual grid points. Also shown is the trailing edge streamline, obtained from integration of the velocity field of the viscous flow. Once again we stress that these smooth results have been obtained straight from the discretization method, without any additional artificial smoothing.

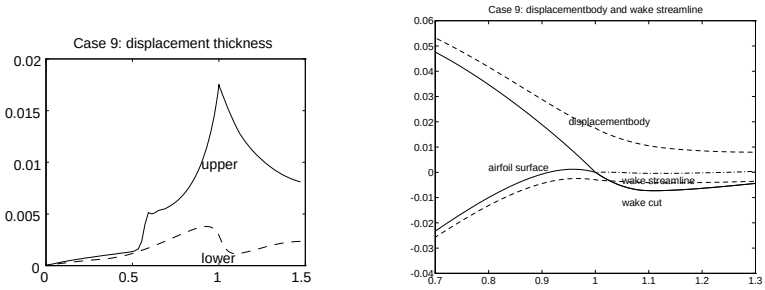

Figure 7. Displacement thickness *(left)* **and displacement body** *(right)* **for RAE2822 - Case 9 (note the enlarged scale in vertical direction).**

C. Comparison with other methods

The present result for Case 6 has been compared in Fig. 8 with results of various VII-methods and Navier–Stokes methods from the Viscous Transonic Airfoil Workshop.[2] Figure 8 shows the scattering of the calculated results for Case 6 to be relatively large, even between the Navier–Stokes methods. An overview of results for Cases 1 and 9 can be found in Ref. 26.

Part of the scattering is due to discretization and solution (iteration) errors, i.e. it is numerical noise. But another important part of the scattering is caused by the difference in turbulence models applied. Coakley[27] focusses on the influence of different turbulence models in Reynolds-averaged Navier–Stokes methods at various flow conditions. Especially when the flow is separated and shocks occur, there is a substantial difference in the calculated flow field. In Fig. 8 his results for Case 6 can be found at $\alpha = 2.40$ (four results, corresponding with four different turbulence models). Coakley's results and those of the other participants in the VTA-Workshop[2] led Holst to the conclusion, already referred to in Section A, that "improved turbulence models are desperately needed."

The extent of these modeling errors remains unevitably unassessed. Even if the numerical noise is minimized, the error due to the lack of physical relevance of the turbulence model cannot be assessed, because no sufficiently accurate experiments are available. Validation of the present results against other digital simulation results is hampered through these unassessed modeling errors. The only judgement that can be expressed here is that the VII results are no better and no worse than those of the more expensive

Navier–Stokes methods. Although the above comparison has been carried out almost two decades ago, in my opinion, since then the progress in turbulence modelling has not yet led to significantly (and systematically) better flow predictions, as demonstrated in more recent reviews.[28,29]

V. The quest for a simpler interaction law

A. A model problem

The implementation of an interaction law, be it the thin-airfoil expressions for thickness (10) and camber (11, 12) or an influence matrix of a panel method, can be cumbersome. Therefore, it is worthwhile to investigate how much the interaction law can be simplified, in the direction of the classical condition 'u_e = prescribed', without being struck by Goldstein's singularity. The viscous-inviscid convergence is likely to deteriorate, but the effort to adapt an existing 'classical' boundary-layer code to separated-flow computations will be smaller. Thus, referring to the quasi-simultaneous formulation (9), the question is

How 'small' can I be chosen?

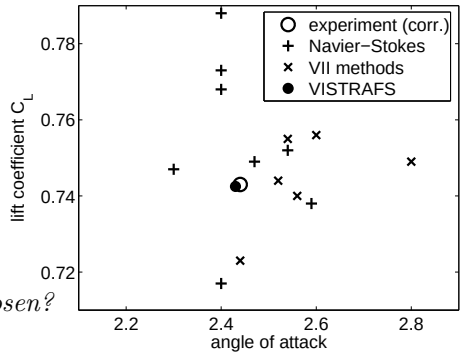

Figure 8. Comparison of present VISTRAFS result for RAE2822 Case 6 ($M_\infty = 0.725, Re = 6.5 \times 10^6$) with VTA workshop[2]

This question has been thoroughly investigated in the Ph.D. thesis of Coenen.[30] She has performed an analysis based on the theory for non-negative matrices and the closely related M-matrices.[31,32] We will first summarize the theory as developed by Coenen; thereafter the usefulness of the theory will be demonstrated on some realistic flow problems. As a reminder, it is remarked that $I = 0$ corresponds with the direct method that blows up in Goldstein's singularity.

To shape the theory, as a model problem the flow past an indented plate is studied for which the external flow will be described by the thin-airfoil expression (10). It is our aim to construct a simple interaction law for this case. Let us first collect some properties of the operators E and B in Eq. (9).

External flow The integral (10) is discretized on a uniform grid with mesh size h. The displacement thickness δ^* is interpolated by a piecewise linear function; only on the two intervals adjacent to the Cauchy principal value a quadratic interpolation is used:

$$\begin{aligned} E\,[\delta^*] \equiv \frac{1}{\pi}\int_\Gamma \frac{\mathrm{d}\delta^*}{\mathrm{d}\xi}\,\frac{\mathrm{d}\xi}{x_i-\xi} &= \frac{1}{\pi}\left\{\int_{x_{i-1}}^{x_{i+1}} + \Sigma_{j\neq i-1,i}\,\frac{1}{\pi}\int_{x_j}^{x_{j+1}}\right\}\frac{\mathrm{d}\delta^*}{\mathrm{d}\xi}\,\frac{\mathrm{d}\xi}{x_i-\xi} \\ &\approx -\frac{2h}{\pi}\left.\frac{\mathrm{d}^2\delta^*}{\mathrm{d}\xi^2}\right|_i + \frac{h}{\pi}\,\Sigma_{j\neq i-1,i}\left.\frac{\mathrm{d}\delta^*}{\mathrm{d}\xi}\right|_{j+1/2}\ln\left|\frac{i-j}{i-j-1}\right| . \end{aligned} \tag{17}$$

After discretization of the ξ-derivatives in Eq. (17), the corresponding discrete matrix $\mathbf{E}$ is symmetric, positive definite with diagonal $4/\pi h$, and with non-positive off-diagonal entries.

Boundary-layer flow Referring e.g. to Ref. 22, a discrete boundary-layer operator $\mathbf{B}$ typically is lower diagonal, with negative diagonal entries for attached flow and (slightly) positive diagonal entries for reversed flow; compare the slope of the (δ^*, u_e)-relation in Fig. 2.

B. Simplified interaction in theory

To develop the theory, first the quasi-simultaneous method (9) will be rewritten in matrix notation

$$\left.\begin{aligned} u_e^{(n)} - \mathbf{I}\,\delta^{*(n)} &= (\mathbf{E}-\mathbf{I})\,\delta^{*(n-1)} \\ u_e^{(n)} - \mathbf{B}\,\delta^{*(n)} &= 0 \end{aligned}\right\} \Rightarrow (\mathbf{I}-\mathbf{B})\,\delta^{*(n)} = (\mathbf{I}-\mathbf{E})\,\delta^{*(n-1)} . \tag{18}$$

After convergence, the ultimate system to be solved reads in matrix notation

$$(\mathbf{E} - \mathbf{B})\ \delta^* = 0\ . \tag{19}$$

We will consider situations with steady flow, for which it is natural to make the following assumption; moreover it allows theory to be developed:

> *Assumption* The matrix $\mathbf{E} - \mathbf{B}$ is assumed to be (positive) stable, i.e. all its eigenvalues lie in the stable half plane, with positive diagonal entries and non-positive off-diagonal entries (hence it is an M-matrix).

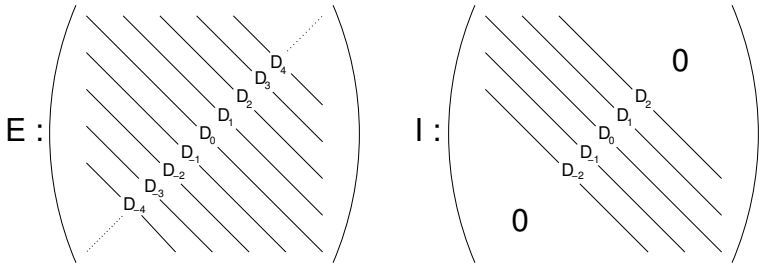

Figure 9. The interaction law I *(right)* may be obtained from the external flow matrix E *(left)* by omitting some off-diagonals (here two diagonals on each side have been retained).

The choice of the interaction law obviously has an influence on the numerical behaviour of the viscous-inviscid algorithm. In the above setting a number of theoretical statements can be made:[30]

1. *VII iterations* An interaction law as in Eq. (18) corresponds with a splitting $\mathbf{E}-\mathbf{B} = (\mathbf{I}-\mathbf{B})-(\mathbf{I}-\mathbf{E})$. When $\mathbf{I} \geq \mathbf{E}$ this splitting is regular, and theory about its convergence is available (Ref. 32, page 88). This suggests to construct $\mathbf{I}$ from $\mathbf{E}$ by dropping one or more off-diagonals (Fig. 9). Subsequently it can be proven that the convergence of the VII iterations deteriorates monotonously with the number of dropped off-diagonals in $\mathbf{I}$.

2. *Boundary-layer iterations* Each VII iteration a boundary-layer computation has to be performed, in which Eq. (18) is to be solved. This is done by repeated, Gauss-Seidel type, marching through the boundary layer, for which a strong diagonal enhances convergence. In this way it can be proven that the Gauss-Seidel convergence improves monotonously with the number of dropped off-diagonals in $\mathbf{I}$.

3. *Robustness* The boundary-layer formulation is highly nonlinear as already shown in Fig. 2. This figure shows that prescribing a linear combination of u_e and δ^*, as is the case when an interaction law is applied, will only be useful when the coefficient of δ^* stays sufficiently away from zero through all stages of the iterative solution process. Hence a large coefficient of δ^* is profitable, or in matrix terms, the eigenvalues of $\mathbf{I} - \mathbf{B}$ should stay sufficiently far from the imaginary axis. In this respect it can be proven that the robustness of the interaction law grows with the number of dropped off-diagonals.

The latter two aspects do suggest to choose the interaction law 'simply' as just the diagonal of the external-flow operator. In contrast, the first aspect suggests to take it equal to the full external-flow operator. The numerical behaviour in practice has to reveal which of the two effects is dominating.

C. Simplified interaction in practice

From a systematic study[30] of turbulent flow along the indented plate, it follows that the above extremes are the most interesting choices for the interaction law. The choice $\mathbf{I} = \mathbf{E}$ would correspond to a fully simultaneous treatment, leaving the choice $\mathbf{I} = \mathrm{diag}(\mathbf{E})$ as the interesting quasi-simultaneous choice.

This choice for an, indeed very simple, interaction law will now be tested for aerodynamic flow past a NACA0012 airfoil (at $Re = 9 \cdot 10^6$, and $M_\infty = 0$); experimental data is available. The inviscid flow is modelled by potential theory, and computed by means of a panel method. Boundary layer plus wake are modelled with Head's entrainment method.[30] They are solved together with the interaction law

$$\mathbf{I} = \mathrm{diag}\{4/\pi h\}\ . \tag{20}$$

We stress that this interaction law is unaware of the Kutta condition and its effect on the global circulation; it only accounts for the local VII physics. But this turns out to be sufficient!

A large part of the lift polar has been computed (Fig. 10). The calculations turn out to be highly robust. It appears that even for separated-flow cases beyond maximum lift the calculations converge without any need for a good initial guess; they can be started from scratch! The number of VII iterations with the extremely simple interaction law (20) typically is less than 100 at zero lift up to 1000 around maximum lift; only for larger angles of attack the computations break down. The number of iterations may sound large, but they can easily can be combined with the time-stepping in an unsteady inviscid-flow solver. Unfortunately, such an unsteady flow solver is not at my disposal, and the evaluation of the performance of the above 'minimal' interaction law (20) in transonic flow conditions will have to wait. Anyway, in the above setting, for two-dimensional simulations the computing times count in just seconds on an average PC. So only in the extension of the method to three dimensions computing times could form an issue. By the way, many three-dimensional quasi-simultaneous experiences have been gathered over the years.[30,33,34,35,36,37,38]

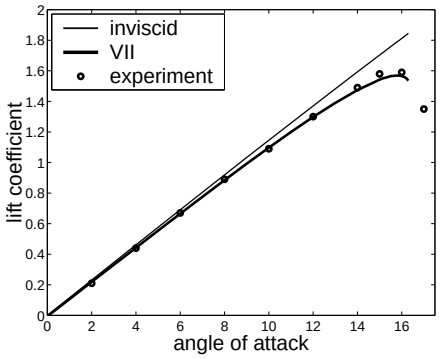

Figure 10. Lift polar for NACA0012 airfoil: viscous-inviscid calculation versus experiment.

VI. Concluding remarks

Mathematics A quasi-simultaneous VII method, originally developed at NLR, has been discussed. A description has been presented of the underlying mathematical model which includes the effect of pressure variations across the shear layer. By modelling the pressure jump across the shear layer in integral formulation the shear-layer equations remain parabolic. In this way the required solution effort remains modest. It is essential for the convergence of the VII iterations that the pressure jump is treated simultaneously with the shear-layer equations. The calculations show a swift convergence of the iterations between the viscous-flow and inviscid-flow solvers. This convergence is found to be independent of the grid size.

Further, a theoretical analysis of the interaction law has been carried out, suggesting a very simple one, and which corresponds to a boundary condition

$$\left(u_e + \frac{4}{\pi h}\,\delta^*\right)^{(\text{new})} = \left(u_e + \frac{4}{\pi h}\,\delta^*\right)^{(\text{old})} .$$

This slight change from the classical formulation, unlikely to be further simplified, results in a highly robust calculation method, applicable to subsonic airfoil calculations beyond maximum lift. Its performance on transonic flow remains to be investigated.

Physics Results from VISTRAFS have been presented for the moderately rear-loaded RAE 2822 airfoil, both with and without modeling of the pressure variations across the shear layer. Both sets of results are comparable to those of other digital simulation methods: VII-methods as well as TLNS-methods. The better agreement with the physical simulation results is obtained when the normal pressure variations have been taken into account. Validation against other digital simulation results is still hampered through the large influence of the turbulence model on the results.

Thus, at present the Navier–Stokes methods do not perform significantly better than VII methods, although the latter require much less computer resources. The current method requires only a price of roughly five times that of a potential flow solver, which is two orders more efficient than a Navier–Stokes solver. As a consequence, the present approach fits easily in a simple PC. As long as turbulence models do not significantly improve, this situation will remain unchanged. Therefore, at the moment VII methods are certainly worth their name: "poor man's Navier–Stokes".

Acknowledgments

Part of this investigation has been performed while the author was employed at the National Aerospace Laboratory NLR in Amsterdam (The Netherlands). The author gratefully acknowledges the contributions of his colleagues Jan Lindhout and Monique Somers at NLR, and Edith Coenen at the University of Groningen.

References

[1]Melnik, R.E., "Turbulent Interactions on Airfoils at Transonic Speeds - Recent Developments," *Computation of Viscous-Inviscid Interactions*, AGARD-CP-291, Feb. 1981.

[2]Holst, T.L., "Viscous Transonic Airfoil Workshop," AIAA Paper 87–1460, June 1987.

[3]Cebeci, T., Clark, R.W., Chang, K.C., Halsey, N.D., and Lee, K., "Airfoils with Separation and the Resulting Wakes," *Proc. 3rd Symposium on Numerical and Physical Aspects of Aerodynamic Flows*, edited by T. Cebeci, Jan. 1985.

[4]Boerstoel, J.W., and Kassies, B., "Integrating Multigrid Relaxation into a Robust Fast-Solver for Transonic Potential Flow Around Lifting Airfoils," AIAA Paper 83–1885, July 1983.

[5]Lock, R.C., and Williams, B.R., "Viscous-Inviscid Interactions in External Aerodynamics," *Prog. Aerospace Sci.*, Vol. 24, 1987, pp. 51–171.

[6]Goldstein, S., "On Laminar Boundary Layer Flow near a Point of Separation," *Quart. J. Mech. Appl. Math.*, Vol. 1, 1948, pp. 43–69.

[7]Catherall, D., and Mangler, K.W., "The Integration of the Two-Dimensional Laminar Boundary-Layer Equations past the Point of Vanishing Skin Friction," *J. Fluid Mech.*, Vol. 26, 1966, pp. 163–182.

[8]Stewartson, K., "On the Flow near the Trailing Edge of a Flat Plate II," *Mathematika*, Vol. 16, 1969, pp. 106–121.

[9]Messiter, A.F., "Boundary-Layer Flow near the Trailing Edge of a Flat Plate," *SIAM J. Appl. Math.*, Vol. 18, 1970, pp. 241–257.

[10]Neiland, V.Ya., "Towards a Theory of Separation of the Laminar Boundary Layer in a Supersonic Stream," *Fluid Dynamics*, Vol. 4, 1970, 33–55.

[11]Lagerstrom, P.A., "Solutions of the Navier–Stokes Equation at Large Reynolds Number," *SIAM J. Appl. Math.*, Vol. 28, 1975, pp. 202–214.

[12]LeBalleur, J.C., "Couplage Visqueux-Non Visqueux: Analyse du Problème Incluant Décollements et Ondes de Choc," *La Recherche Aérospatiale*, Vol. 1977-6, 1977, pp. 349–358.

[13]LeBalleur, J.C., "Couplage Visqueux-Non Visqueux: Méthode Numérique et Applications aux Écoulements Bidimensionnels Transsoniques et Supersoniques," *La Recherche Aérospatiale*, Vol. 1978-2, 1978, pp. 65–76.

[14]Carter, J.E., "Viscous-Inviscid Interaction Analysis of Turbulent Separated Flow," AIAA paper 81–1241, June 1981.

[15]LeBalleur, J.C., "New Possibilities of Viscous-Inviscid Numerical Techniques for Solving Viscous Flow Equations with Massive Separation," *Numerical and Physical Aspects of Aerodynamic Flow IV*, edited by T. Cebeci, Springer Verlag, Berlin, 1990, pp. 71–96.

[16]Veldman, A.E.P., "A Numerical Method for the Calculation of Laminar Incompressible Bounday Layers with Strong Viscous-inviscid Interaction," National Aerospace Laboratory, Report NLR TR 79023, Amsterdam, 1979.

[17]Veldman, A.E.P., "New Quasi-simultaneous Method to Calculate Interacting Boundary Layers," *AIAA Journal*, Vol. 19, 1981, pp. 79-85.

[18]Moses, H.L., Jones III, R.R., O'Brien Jr., W.F., and Peterson, R.P., "Simultaneous Solution of the Boundary Layer and Freestream with Separated flow," *AIAA Journal*, Vol. 16, No. 1, 1978, pp. 61–66.

[19]Houwink, R., and Veldman, A.E.P., "Steady and Unsteady Separated Flow Computation for Transonic Airfoils," AIAA Paper 84–1618, June 1984.

[20]Drela, M., and Giles, M.B., "Viscous-Inviscid Analysis of Transonic and low Reynolds Number Airfoils," *AIAA Journal*, Vol. 25, No. 10, 1987, pp. 1347–1355.

[21]Dargel, G., and Thiede, P., "Viscous Transonic Airfoil Flow Simulation by an Efficient Viscous-Inviscid Interaction Method," AIAA Paper 87–0412, Jan. 1987.

[22]Veldman, A.E.P., ' 'A Numerical View on Strong Viscous-inviscid Interaction," *Computational Methods in Viscous Flow*, edited by W.G. Habashi, Pineridge Press, Swansea, 1984, pp. 343–364.

[23]Veldman, A.E.P., Matched Asymptotic Expansions and the Numerical Treatment of Viscous-inviscid interaction, *J. Engng Math.*, Vol. 39, 2001, pp. 189–206.

[24]Veldman, A.E.P., and Somers, M.A.M., "The Inclusion of Streamline Curvature in a Quasi-Simultaneous Viscous-Inviscid Interaction Method for Transonic Airfoil Flow," URL: http://www.math.rug.nl/∼veldman/preprints.html, 1999.

[25]Veldman, A.E.P., Lindhout, J.P.F., and de Boer, E., *VISIAN: A Viscous-Inviscid Strong-Interaction Analysis System*, National Aerospace Laboratory, NLR Report TR 88081, 1988.

[26]Veldman, A.E.P., Lindhout, J.P.F., de Boer, E., and Somers, M.A.M., "VISTRAFS: A Simulation Method for Strongly-Interacting Viscous Transonic Flow," *Numerical and Physical Aspects of Aerodynamic Flow IV*, edited by T. Cebeci, Springer Verlag, Berlin, 1990, pp. 37–51.

[27]Coakley, T.J., "Numerical Simulation of Viscous Transonic Airfoil Flows," AIAA Paper 87–0416, Jan. 1987.

[28]Haase, W., Brandsma, F., Elsholz, E., Leschziner, M., and Schwamborn, D. (eds.), *EUROVAL — An European Initiative on Validation of CFD Codes*, Notes on Numerical Fluid Mechanics 42, Vieweg Verlag, Braunschweig, 1993.

[29]Agarwal, R., "Computational Fluid Dynamics of Whole-Body Aircraft," *Ann. Rev. Fluid Mech.*, Vol. 31, 1999, pp. 125–169.

[30]Coenen, E.G.M., "Viscous-Inviscid Interaction with the Quasi-Simultaneous Method for 2D and 3D Airfoil Flow," Ph.D. Dissertation, University of Groningen, 2001, URL: www.ub.rug.nl/eldoc/dis/science/e.g.m.coenen.

[31]Horn, R.A., and Johnson C.R., *Topics in Matrix Analysis*, Cambridge University Press, Cambridge, UK, 1991.

[32]Varga, R.S., *Matrix Iterative Analysis*, Prentice-Hall, Englewood Cliffs, New Jersey, 1962.

[33]Edwards, D.E., "Analysis of Three-Dimensional Separated Flow Using Interacting Boundary-Layer Theory," *Boundary-Layer Separation,* edited by F.T. Smith and S.N. Brown, Springer Verlag, Berlin, 1987, pp. 163–178.

[34]Smith, F.T., "Steady and Unsteady 3-d Interactive Boundary Layers," *Comp. Fluids*, Vol. 20, 1991, pp. 243–268.

[35]van der Wees, A.J., and van Muijden, J., "A Fast and Robust Viscous-Inviscid Interaction Solver for Transonic Flow about Wing/Body Configurations on the Basis of Full Potential Theory," AIAA Paper 93–3026, 1993.

[36]Roget, C., Brazier, J.Ph., Cousteix, J., and Mauss, J., "A Contribution to the Physical Analysis of Separated Flows past Three-Dimensional Humps," *Eur. J. Mech. B*, Vol. 17, 1998, pp. 307–329.

[37]Cebeci, T., *An Engineering Approach to the Calculation of Aerodynamic Flows*, Springer Verlag, Berlin, 1999.

[38]Coenen, E.G.M., "Quasi-Simultaneous Coupling for Wing and Airfoil Flow," *Domain Decomposition Methods in Science and Engineering*, edited by C.-H. Lai, P.E. Bjorstad, M. Cross and O.B. Widlund, Domain Decomposition Press, Bergen, 1999, pp. 197–205.